Supporting Information

Contact line dynamics modulated by electrode roughness determines bubble detachment size

Weikang Yang[a,*], Dongxu Gu[b], Xin Liu[a], Qiangmin Luo[a]

[a] *School of Chemistry and Chemical Engineering, Chongqing University, Chongqing 400044, PR China.*

[b] *Institute of Intelligent Innovation, Henan Academy of Sciences, Zhengzhou, Henan, 451162, P. R. China.*

*Corresponding author. *E-mail: wkyang@stu.cqu.edu.cn; Phone: +86 18725737346.*

1. Electrode Preparation

The nickel (Ø500 μm) wire-welded copper leads were fixed onto a pre-assembled square frame (Fig. S1). Epoxy resin was prepared by mixing component A and B at a mass ratio of 2:1. Vigorous stirring introduced numerous microbubbles, resulting in an opaque, milky-white mixture. To eliminate entrapped bubbles, the epoxy was centrifuged until achieving optical clarity and high fluidity. After 30 minutes of static curing at ambient temperature (28°C), the resin's viscosity increased moderately, at which point it was poured into the frame to encapsulate the electrode. Additional epoxy layers could be applied within 1 hour to ensure complete coverage of both nickel wire and copper leads. The assembly was then cured at room temperature for 12 hours before frame removal. Finally, polished edges were created on the cured epoxy block to facilitate subsequent experimental observations.

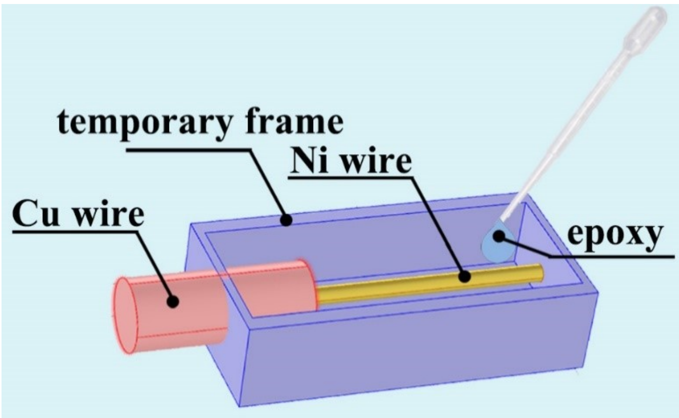

Fig. S1. Schematic of the electrode package.

The subsequent Ni electrodes working face was directly polished using sandpaper (wuxi-1200, wuxi-800 and wuxi-400) to prepare three representative Ni electrodes with varying surface roughness, which were utilized as working electrodes. While our embedded electrode design enables precise observation of bubble dynamics, it inherently creates lateral inhomogeneity in electrochemical rates. As noted in recent studies[1,2], such inhomogeneity may induce density-driven convection. Although this effect does not alter our primary conclusions on contact line dynamics, future work could explicitly quantify its influence through computational fluid dynamics simulations.

2. Image Analysis

The image analysis program was developed based on the image processing module of MATLAB (R 2022b). Firstly, the background was subtracted, and then the contrast and brightness were adjusted for further binarization. Fig. S2a and S2b present the bubble images after contrast enhancement and binarization processing, respectively. To quantify the contact line dynamics, edge coordinates were extracted from the processed images using computational algorithms, as demonstrated by the scatter plot in Fig. S2c. The bottom radius and contact angle of the bubble were subsequently determined through statistical analysis of the spatial distribution characteristics of these edge coordinate points.

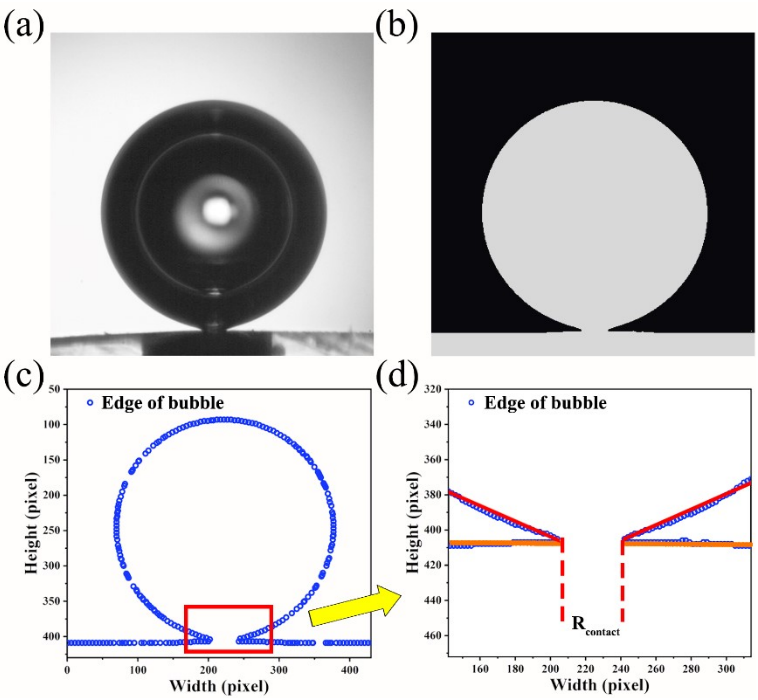

Fig. S2. (a) the original image with contrast enhancement; (b) the binarized image; (c) Scattered data at the edges; (d) Scatter points used to fit the baseline and tangents.

To verify the accuracy of our custom-developed algorithm, we compared its contact angle calculations with those obtained from commercial contact angle measurement software (SCA20) at multiple time points. As illustrated in Fig. S3a, representative images from the commercial software's fitting process are displayed (three typical examples shown), while Fig. S3b presents the complete dataset comparison between both methods. The custom algorithm demonstrated consistent reliability throughout the measurement period, with a maximum deviation of less than 2° compared to the commercial software. Notably, the automated processing capability of our custom program addressed the critical limitation of the commercial software, which could only perform manual frame-by-frame analysis - a method unsuitable for our high-throughput experimental requirements.

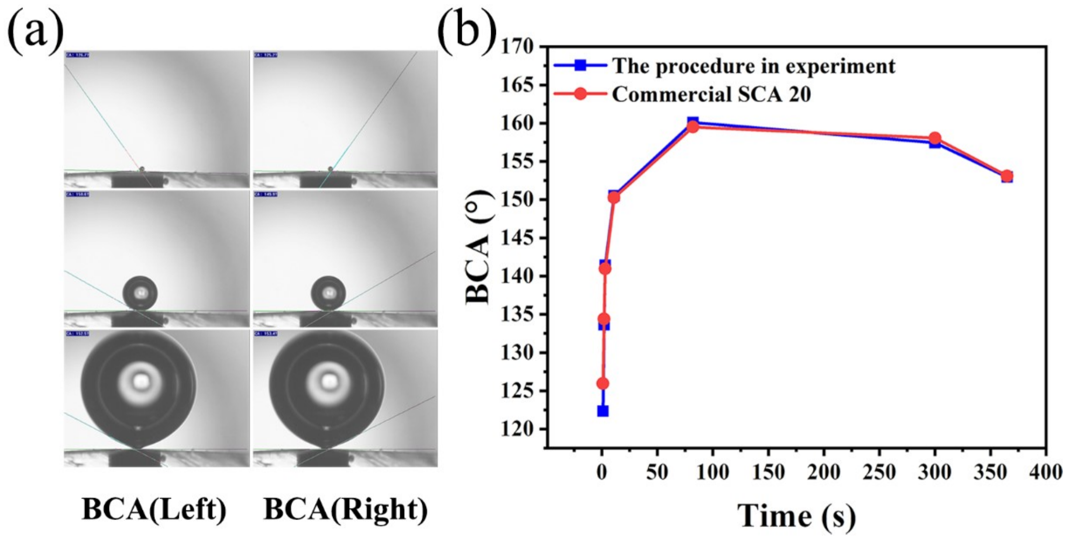

Fig. S3. (a) Commercial software SCA20 to measure the contact angle; (b) Comparison of contact angles obtained by the program and results obtained by commercial software.

3. Contact line dynamics at different current densities

To investigate potential current density effects on hydrogen bubble adhesion dynamics, we first examined bubble growth patterns on the smoothest Ni electrode surface (M1). Fig. S4a presents processed images of the bubble growth process, clearly showing neck formation during expansion. The radius-time curves in Fig. S4b reveal that as the current density increases, the bubble detachment size grows from 513 μm to 551 μm, corresponding to an approximately 24% increase in additional buoyancy force. This suggests that the current density generates an additional downward force. As demonstrated by Park et al.[3], the ion concentration gradient generated near the electrode induces solutal Marangoni flow, which exerts an additional downward force on the bubble (in sulfuric acid electrolyte). The elevated current density leads to increased ion concentration gradients, which may explain the slightly larger detachment sizes observed in our experiments. Notably, higher current densities accelerated bubble growth rates due to enhanced hydrogen generation, leading to greater molecular hydrogen concentration gradients and interfacial mass transfer fluxes at the electrode surface. Contact line dynamics (Fig. S4c) exhibited universal characteristics regardless of current density: rapid expansion to a maximum radius of 90 μm, followed by gradual contraction to 70 μm at detachment. Similarly, contact angles (Fig. S4d) demonstrated consistent evolution - rapid increase to 160°, stabilization, then decline to ~150° at detachment.

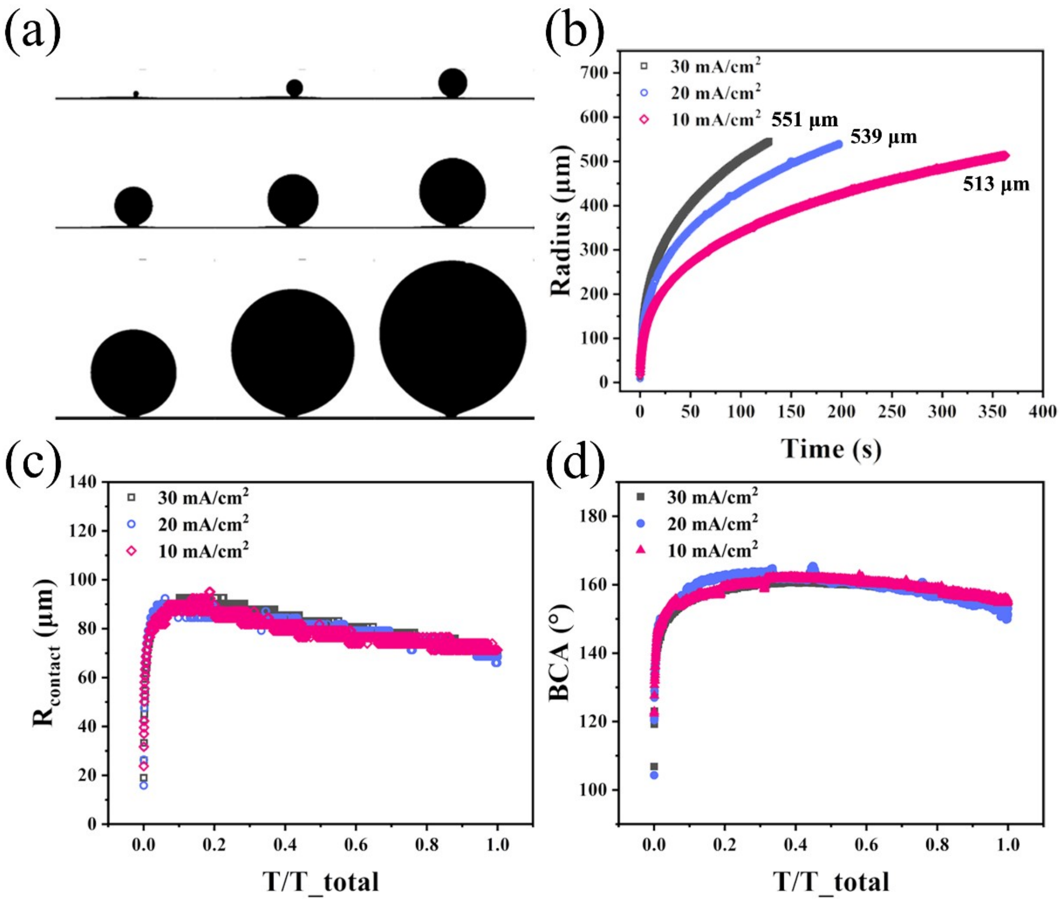

Fig. S4. (a) Commercial software SCA20 to measure the contact angle; (b) Comparison of contact angles obtained by the program and results obtained by commercial software.

Fig. S5 presents the bubble contact line parameters normalized by bubble size to eliminate temporal effects. The size-normalized analysis reveals remarkable consistency in contact line behavior across different current densities. As shown in Fig. S5a, the contact radius initially increases with bubble growth, reaching a maximum value of 94 μm at a bubble size of 253 μm, after which further bubble expansion leads to contact line contraction. The dynamic contact angle evolution (Fig. S5b) similarly demonstrates current-density-independent characteristics, beginning to decrease when the bubble reaches 377 μm in size. These findings conclusively demonstrate that the contact line evolution on a given electrode surface is governed by surface topography and the resultant force balance, rather than being influenced by current density variations.

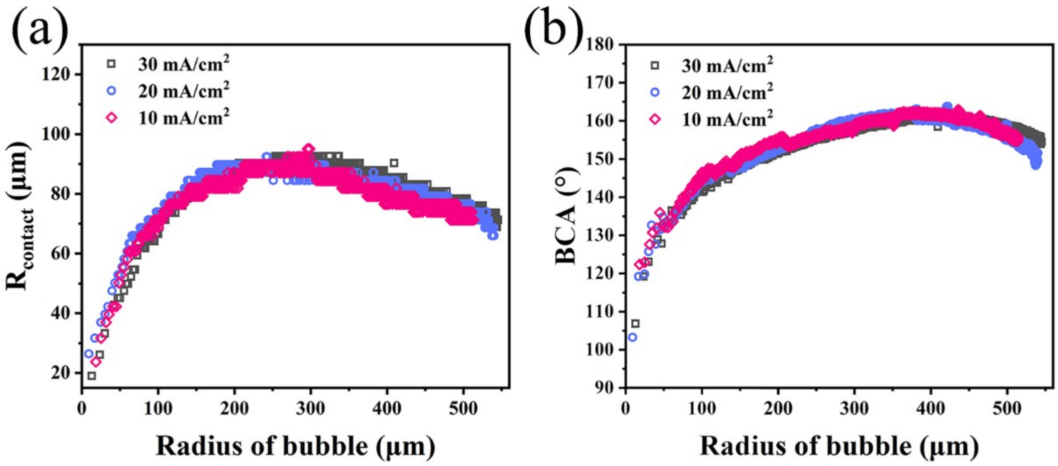

Fig. S5. Under different current densities: (a) Relationship between contact radius and bubble size; (b) Relationship between dynamic contact Angle and bubble size.

Fig S6 presents the Ni electrode surface morphology before and after HER using quasi-in situ AFM measurements during 10 min of electrolysis at 20 mA/cm², revealing only marginal roughness increases (M1: 5.64→5.69 nm; M2: 8.73→8.97 nm; M3: 13.88→14.32 nm) that confirm negligible structural modifications, while the bubble behavior appears dominated by initial surface roughness rather than these minimal HER-induced changes due to the orders-of-magnitude larger bubble dimensions compared to roughness variations.

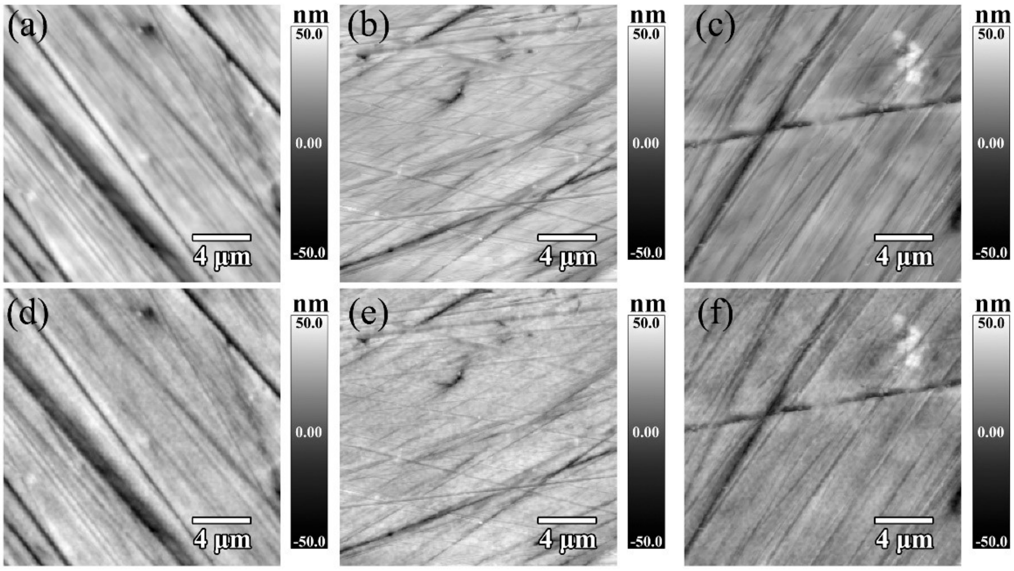

Fig. S6. Two-dimensional morphology of nickel electrode before HER: (a) M1, (b) M2, (c) M3; Two-dimensional morphology of nickel electrode after HER: (d) M1, (e) M2, (f) M3.

References

[1] H. M. Rodriguez, M. Martyniuk, K. S. Iyer and S. Ciampi, *J. Am. Chem. Soc.* 2024, ***146***, 10299-10311.

[2] V. Sahore, A. Kreidermacher, F. Z. Khan and I. Fritsch, *J. Electrochem. Soc.* 2016*,* ***163,*** H3135.

[3] S. Park, L. Liu, Ç. Demirkır, O. Heijden, D. Lohse, D. Krug and M. T. M. Koper, *Nat. Chem.*, 2023, ***15***, 1532-1540.